

however, an enol structure as the basic form of the compound in dilute benzene solution, the calculated moment of α -hydroxycyclohexanone is found to be in the range of 2.8–3.0D. This value is in good agreement with the experiment. Free rotation of the enolic form is eliminated on the basis of the same reasoning as used for the 1,2 diols. Infrared spectra²¹ of the vacuum distilled liquid used in run no. 2 showed the presence of appreciable amounts of the carbonyl group and hence the liquid must be quite rich in the ketonic form. In benzene solution, however, the vacuum distilled liquid gave essentially the same experimental moment as the solid form used for run no. 1. Thus it may be concluded that α -hydroxycyclohexanone exists in benzene solution as a

mixture of isomers with the enolic form predominating.

Summary

1. The electric moments of *cis*-cyclohexanediol-1,2, *trans*-cyclohexanediol-1,2, *cis*-cyclohexanediol-1,4, *trans*-cyclohexanediol-1,4, cyclohexanedione-1,2 and α -hydroxycyclohexanone have been determined in benzene and are equal to 2.33, 2.39, 2.50, 1.80, 2.80, and 2.90D, respectively.

2. Limited conclusions as to the configurations of these compounds in benzene solution have been drawn on the basis of general theory and the experimental results.

COLLEGE PARK, MARYLAND

RECEIVED DECEMBER 15, 1949

[CONTRIBUTION FROM THE DEPARTMENT OF CHEMISTRY OF THE ILLINOIS INSTITUTE OF TECHNOLOGY]

The Oxidation of Several Metals in Activated Oxygen at High Temperatures^{1,2}

BY ANDREW DRAVNIKS³

Introduction.—Heretofore kinetic studies on the oxidation of metal surfaces have been restricted to the use of free oxygen, or some oxidizing compound such as water vapor, carbon dioxide, oxides of nitrogen or ozone. Since it is well known that a properly regulated electric discharge can produce large quantities of oxygen atoms, it seemed worth while to ascertain experimentally the influence of such activated oxygen on the rate of oxidation of copper and other metals. The present paper reports a series of such measurements in the pressure range 0.5 to 2.0 mm. and at temperatures ranging from 500 to 690°.

Experimental

A continuous stream of activated oxygen⁴⁻¹⁰ was produced in the apparatus shown in Fig. 1. The oxygen pressure was maintained within ± 0.05 mm. in the range of pressures of 0.5–4.0 mm.; the linear flow rate of oxygen was 40–70 cm. per second, depending on the pressure of oxygen in the system. The electrical discharge through the activation tube was obtained by means of a 15 kv. transformer, and a current strength up to 68 ma. was employed.

The concentration of oxygen atoms^{11,12} was measured

(1) This research was generously supported by the U. S. Navy Office of Naval Research.

(2) From a thesis submitted to the Illinois Institute of Technology in partial fulfillment of the requirements for the degree of Doctor of Philosophy.

(3) Standard Oil Company (Indiana), Chicago, Illinois.

(4) P. Harteck and U. Kopsch, *Z. physik. Chem.*, **A139**, 98 (1928).

(5) P. Harteck and U. Kopsch, *Z. Elektrochem.*, **36**, 714 (1930).

(6) E. Wrede, *Z. Instrumentenk.*, **48**, 201 (1928).

(7) K. H. Geib, *Erg. Naturwissensch.*, **15**, 80 (1936).

(8) L. C. Copeland, *THIS JOURNAL*, **52**, 2580 (1930).

(9) W. H. Rodebush and S. M. Troxel, *ibid.*, **52**, 3467 (1930).

(10) W. H. Rodebush, *Chem. Rev.*, **17**, 409 (1935).

(11) Gas withdrawn from the experimental space through a narrow glass tube (to effect recombination of the oxygen atoms) imparted very slight color to a potassium iodide-starch-glycerol paper. Ozone introduced into the system caused immediate coloration. Thus the concentration of ozone in the activated oxygen was negli-

gible. The absence of ozone in activated oxygen has been observed previously^{4,6} and explained by the low probability of the triple collisions necessary for the formation of ozone. The rate of decay of the "activity" of the activated oxygen is less than exponential with increase of distance downstream from the discharge. By extrapolation, one may estimate that 30% of the oxygen molecules are dissociated to atoms in the discharge.

(12) Measurements of the conductivity of the gas were made using a galvanometer in series with a 135 v. battery and two copper plates placed parallel 0.4 cm. apart in the experimental space. Within the limits of measurement (10^{-7} amp.) no current was observed so that the concentration of gaseous ions was at most negligible.

(13) Selected Values of Thermodynamic Constants, Natl. Bureau of Standards, Washington, D. C., 1947.

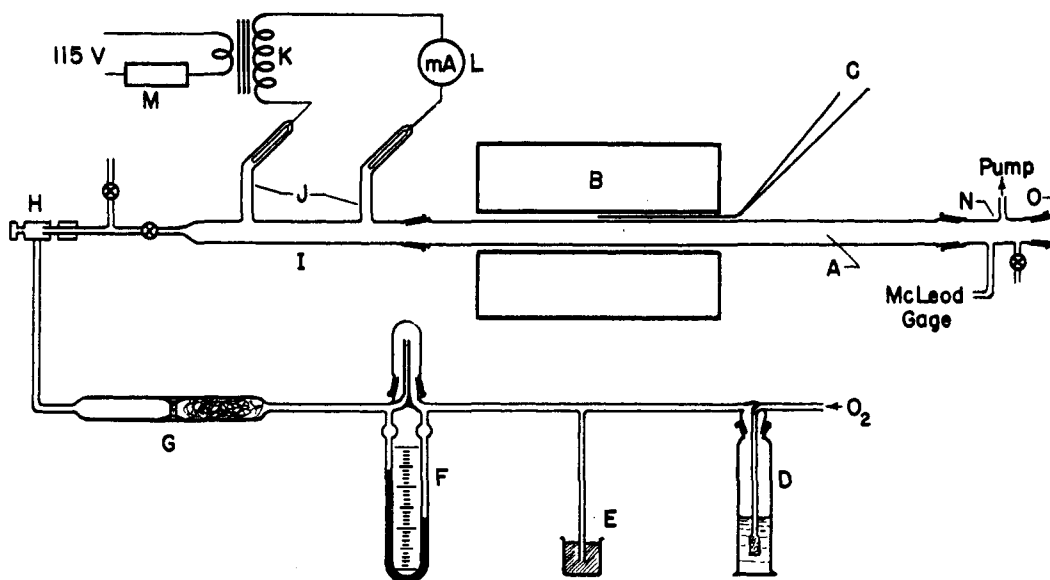


Fig. 1.—The system used for oxidizing metals in activated oxygen: A, silica glass tube; B, furnace; C, thermocouple; D, sulfuric acid bottle; E, Amoil manostat; F, Amoil flowmeter; G, porous glass filter; H, Hoke vacuum needle valve; I, activation tube coated with phosphoric acid; J, side arms with sealed-in aluminum electrodes; K, high voltage transformer; L, milliammeter; M, variable transformer; N, glass piece with connections; O, removable plug. The furnace temperature was kept within better than $\pm 1^\circ$ with a Micromax controller.

The progress of the oxidation of metal strip specimens was continuously followed conductometrically.^{14,15} The equipment is shown schematically in Fig. 2. The size, shape and position of specimens relative to the discharge tube were matched closely to those of the platinum strip used as the atom detector, so that the data on atom concentrations could be applied to the specimens directly. A multipoint recording potentiometer with a ninety second recording cycle recorded the increase of the potential drop along the middle 21 mm. long section of the metal strip as well as the potential drop across a fixed resistance in series with the specimen. Thus a check on the drift of the current strength through the specimen with time was possible. The increase of the resistance of the middle section of the strip and hence the thickness of metal converted to oxide at any moment could be calculated from the recorded data. The penetration of oxide into the metal proceeded fairly uniformly over the surface. The maximum sensitivity of the method at penetration values is equal to one third the thickness of the metal strip used. For copper, the maximum variation did not exceed $\pm 2\%$ at this optimum penetration.

Two or more runs were made under each set of conditions. The average penetrations for various lengths of oxidation were calculated and employed for drawing the oxidation curves.

Copper oxide samples were examined by X-ray techniques and analyzed for cuprous oxide content after removal from the specimens. The analyses were made gas-volumetrically by the determination of the amount of oxygen necessary to oxidize an oxide sample completely to cupric oxide. If only small amounts of scale were available, powder X-ray patterns were microphotometered and compared with those of known mixtures; this procedure was accurate to $\pm 5\%$ as to the content of cupric oxide in the scale. A visual inspection was sufficient to determine whether the scale consisted of only cuprous oxide, since the scale was pure reddish in such a case. As soon as traces of cupric oxide appeared, the surface of the scale

became grey. Thus the color of the scale surface served as a sensitive test to detect the point where cupric oxide starts to form on the surface of cuprous oxide.

Electrolytic copper sheet of 99.8% purity was used; the strip was heated for approximately fifteen minutes at the temperature of the experiment under vacuum before the run was started, and the surface of the copper strip was bright and shiny after this pre-treatment. Other metals were of commercial purity.

Results.—The oxidation curves of copper are presented in Figs. 3, 4 and 5. The oxidation of copper at several values of the activating current through the discharge tube is illustrated by

TABLE I
PARTIAL PRESSURES OF OXYGEN ATOMS AT EXPERIMENTAL CONDITIONS

Conditions Temp., °C.	Press., mm.	Partial pressure of atoms in ord. oxygen, from diss. equilibrium, in 10^{-16} atm.	Partial pressure of excess atoms introduced with active oxygen, in 10^{-8} atm. ^a
500	0.5	0.65	160
	1.0	0.9	74
	2.0	1.3	(8) ^b
600	0.5	65	110
	1.0	90	55
	2.0	130	(5) ^b
690	0.5	2040	80
	1.0	2900	41
	2.0	4100	(4) ^b

^a From the variation of O concentration with pressure, flow rate, temperature, discharge current, and distance from discharge it can be estimated that the values are accurate to $\pm 20\%$ at 500° and less accurate at higher temperatures. ^b The values in parentheses are estimated from the variation of atom concentration with pressure at room temperature; direct measurements at high temperatures were not possible.

(14) W. G. Palmer, *Proc. Roy. Soc. (London)*, **A103**, 444 (1923).

(15) R. R. Seeber, Symposium of Corrosion Testing Procedures, ASTM, 1937.

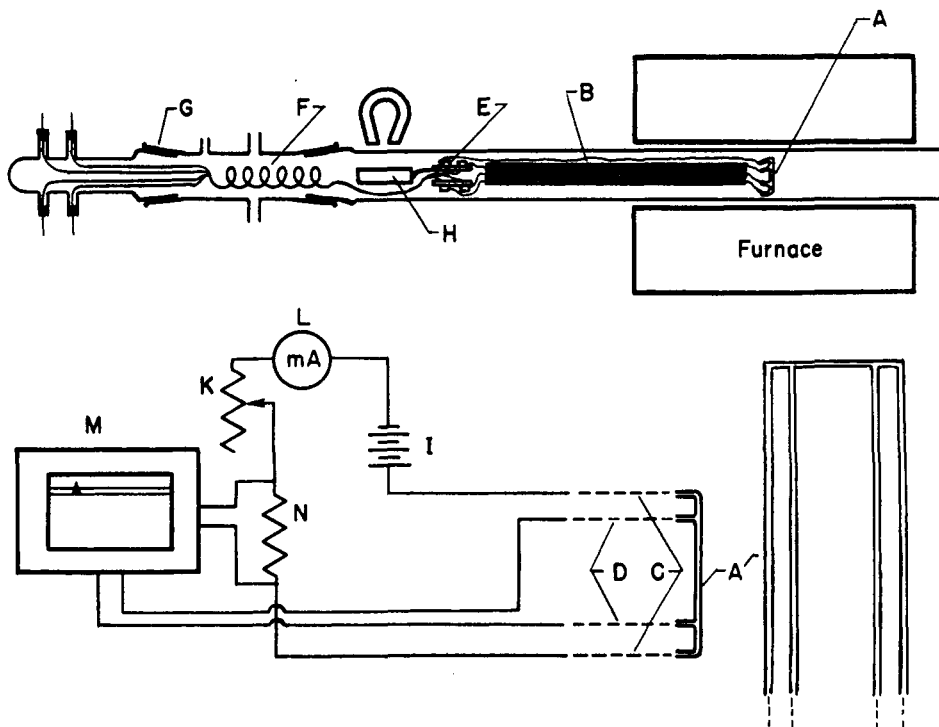


Fig. 2.—Schematic representation of the conductometric apparatus: A, the specimen, cut from one piece of a metal sheet; B, silica glass frame for fixing specimen leads; C, current leads; D, potential pick up leads; E, Plexiglass strips on frame, with screws for wire and specimen leads connections; F, four Formvar enameled flexible copper connection wires; G, standard taper joint, sealed with DeKhotinsky cement; H, iron piece for moving the device into the furnace; I, storage battery; K, N, resistances; L, milliammeter; M, Brown Elektronik 6-point recording potentiometer.

Fig. 6. The oxidation curves of several other metals are shown in Fig. 7. In each plot the ordinate is the square of the depth of penetration. If the parabolic rate law¹⁶⁻¹⁹ is obeyed, the curves are straight. The concentrations of oxygen atoms in ordinary oxygen, as calculated from the dissociation equilibrium of oxygen, and in activated oxygen, as measured with the platinum strip device, are shown in Table I.

Discussion.—In the oxidation of copper both cupric and cuprous oxide are thermodynamically possible reaction products under the conditions studied. However, the color of the scale, the analyses, and the X-ray patterns indicated clearly that at the beginning of the oxidation only cuprous oxide was formed. Cupric oxide appeared only at more advanced stages of oxidation.

At 500° the oxidation curves (Fig. 3) may be fairly well expressed as two straight lines with an intermediate region of rapidly changing slope.

(16) N. B. Pilling and R. E. Bedworth, *J. Inst. Metals*, **29**, 529 (1923).

(17) G. Tammann, *Z. anorg. allgem. Chem.*, **111**, 78 (1920).

(18) C. Wagner and K. Gruenewald, *Z. physik. Chem.*, **B40**, 455 (1938).

(19) From the parabolic law, $dy/dt = k/t$ or $y^2 = 2kt$, plots of y^2 versus t , or t/y versus y are straight lines. Here y is the amount of reaction, *i. e.*, penetration, t is the time from beginning of the reaction, and k is the parabolic rate constant.

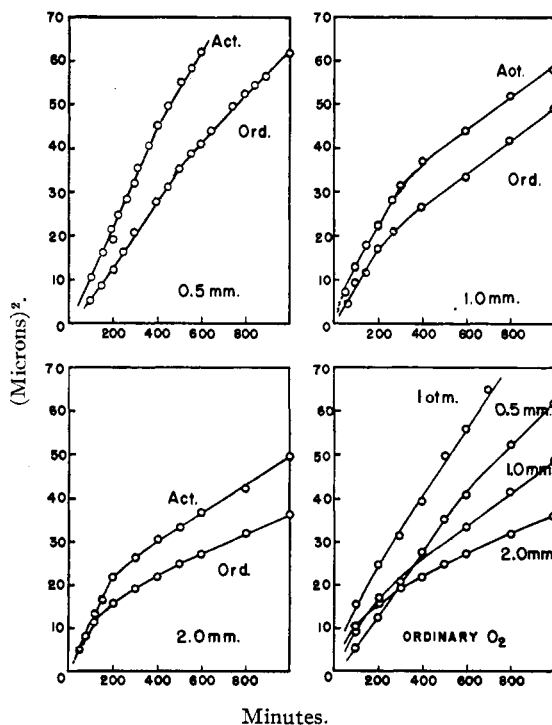


Fig. 3.—Oxidation of copper at 500°.

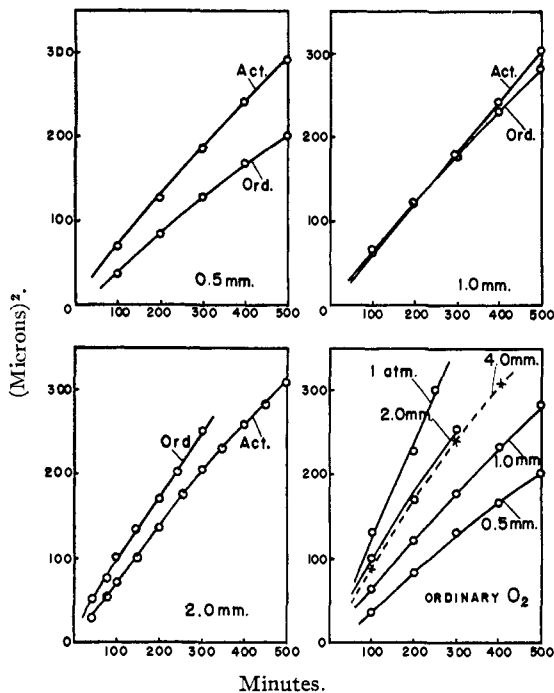


Fig. 4.—Oxidation of copper at 600°.

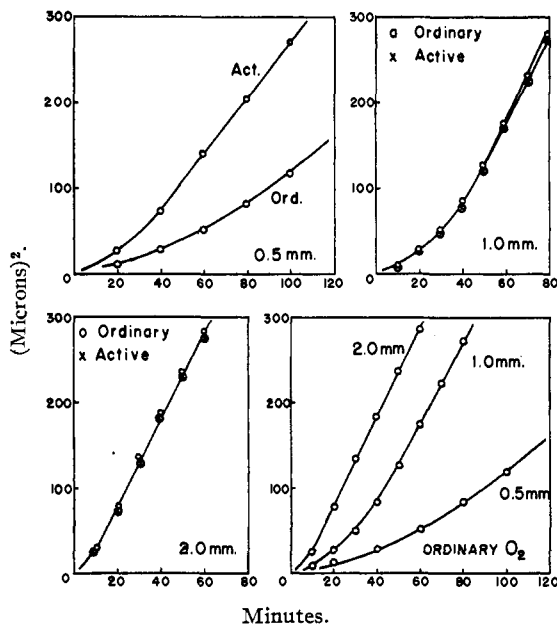


Fig. 5.—Oxidation of copper at 690°.

This character of the oxidation curves is best seen, however, if the data are plotted¹⁹ as in Fig. 8. The plot emphasizes the change in the rate constants which are here proportional to the reciprocal of the slopes. The numbers on the top of the figure indicate percentage cupric oxide in the scale for different degrees of penetration. In the first straight line region only cuprous oxide was detected. In the second region both cuprous and

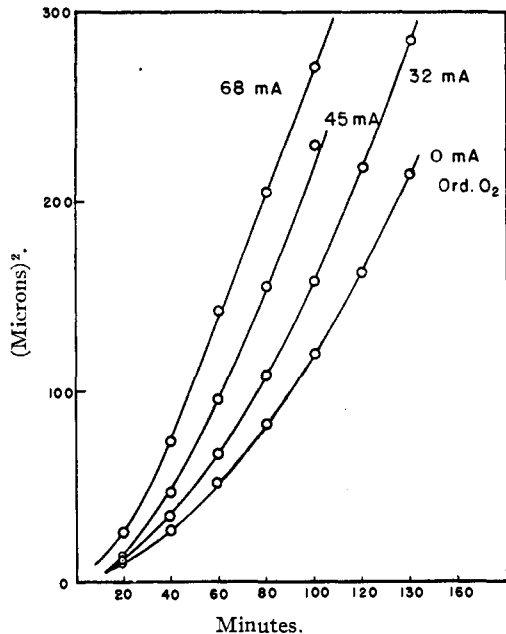


Fig. 6.—Oxidation of copper at 690° and 0.5 mm. pressure: change in rate with variation in activating current.

cupric oxides were invariably present. The mean parabolic rate constants obtained from several runs for each set of conditions are shown in Table II. The rate of oxidation in the first region increases with oxygen pressure. In ordinary oxygen the variation of the first parabolic rate constant with oxygen pressure is of the same magnitude as found by Wagner and Gruenewald¹⁸ for copper at 1000° and for low oxygen pressure where cuprous oxide is the only thermodynamically stable product.

TABLE II
OXIDATION OF COPPER AT 500°

Total oxygen pressure, P mm.	Form of oxygen	Parabolic rate constant ^a $k_1 \times 10^{10}$ $k_2 \times 10^{10}$	Critical thickness d microns ^b $\times 10^{13}$	$k_1/d^2 \times 10^{11}$	$\sqrt{Pd}/k_1 \times 10^{11}$
0.5	Ord.	0.060 0.045	5.8	10	7
	Act.	.090 Indistinct	6.7	14	
1.0	Ord.	.072 0.32	4.2	17	6
	Act.	.097 .030	5.9	17	
2.0	Ord.	.082 .020	3.8	22	7
	Act.	.095 .027	4.9	20	

^a Rate constants in sq. cm. sec.⁻¹. ^b Critical thickness of penetration is the penetration in the middle of the region where the slope of the oxidation curves changes rapidly; obtained from plots like Fig. 8. ^c This ratio is proportional to the rate of arrival of copper ions at the surface of the cuprous oxide scale when cupric oxide starts to precipitate.

From the above evidence, at 500° it seems possible to identify: (1) the first parabolic rate with oxidation to cuprous oxide, (2) the region of the rapidly changing slope with beginning of precipitation of cupric oxide on the surface of the cuprous

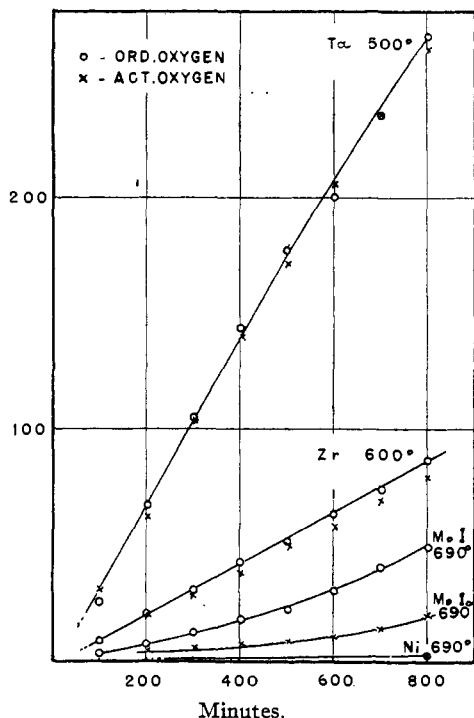


Fig. 7.—Oxidation of several metals at 0.5 mm. oxygen pressure. The ordinate here expresses a combined effect of a change in resistance caused by diffusion of oxygen into the metal and by a decrease in the cross-section of the metal phase. The first factor is especially important for zirconium and tantalum, but probably negligible for nickel. Ordinate is (decrease in the conductivity)², in arbitrary units.

oxide, and (3) the second parabolic region with oxidation which occurs when both oxides are present.²⁰

The penetration at the apparent break in the curves, as obtained from plots such as in Fig. 8, is shown in Table II. From the first parabolic rate constant and the critical thickness of penetration one can calculate the rate of arrival of copper ions at the surface of the cuprous oxide scale when cupric oxide starts to precipitate.²¹ If the square root of oxygen pressure in ordinary oxygen is divided by the calculated rate of arrival of copper ions, the ratio is approximately constant, as indicated by the column headed \sqrt{Pd}/k_1 in Table II. The square root of oxygen pressure is proportional to the concentration of oxygen atoms. Thus in ordinary oxygen the precipitation of higher oxide starts at approximately the same surface conditions if one assumes that the oxygen atoms tend

(20) The breaks in the curves occur too regularly to be explained by Evans' mechanism of blistering; compare U. R. Evans, *Trans. Am. Electrochem. Soc.*, **91**, 547 (1947).

(21) The magnitude of $dy/dt = k/y$ where k is the first rate constant¹⁹ and y the thickness at the apparent break in the curve is proportional to the rate of arrival. Multiplying by GN/A , one could obtain the rate of arrival expressed as number of copper ions arriving per second per sq. cm. of the oxide scale surface. Here G is the density, and A the atomic weight of copper; N is the Avogadro number.

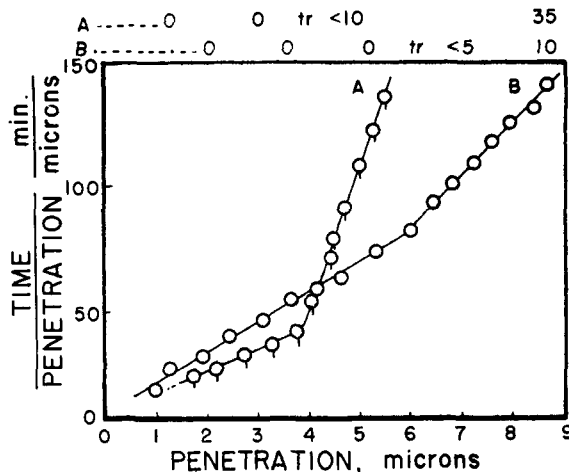


Fig. 8.—Oxidation of copper at 500°: plots of two individual runs in coordinates emphasizing the position of the "critical penetration" value: A, ordinary oxygen at 2.0 mm.; B, ordinary oxygen at 0.5 mm. pressure; the numbers on the top represent per cent. fractions of cupric oxide in the scale at progressing oxidation, for conditions A and B, respectively; "tr" denotes trace.

to precipitate cupric oxide but the arriving copper ions tend to prevent cupric oxide formation.

At 500° in ordinary oxygen the first parabolic rate constant increases with oxygen pressure. By activating the oxygen this constant increases to approximately the same value for all three oxygen pressures. The second parabolic rate constant decreases with an increase in oxygen pressure and is not influenced by activated oxygen. The fraction of cupric oxide in the scale also increases with oxygen pressure if scales at the same penetration value are compared. Activated oxygen at 500° does not accelerate precipitation of cupric oxide. The precipitation seems to occur at the same rate of arrival (Table II) of copper ions as in ordinary oxygen at the same total pressure. Owing to the larger first parabolic rate constant, this occurs, however, at a correspondingly greater thickness.

The rate constants at one atmosphere pressure are not consistent with the pressure dependence of the rate constants at 0.5–2.0 mm. pressures. This may be due to the difference in the behavior of the cuprous oxide layer. This layer is thick when formed at low pressures but relatively thin when formed at atmospheric pressure. In the latter case 95% of the scale consists of cupric oxide covering the cuprous oxide layer.

At 600° the oxidation curves, in most cases, cannot be resolved into two distinct parabolas, although cupric oxide again appears in the scale only after some thickness of scale is formed. At 0.5 mm. pressure the curves in Fig. 4 represent only the cuprous oxide region, and activated oxygen definitely accelerates oxidation. At 1.0 mm., there is no difference in oxidation in the two forms of oxygen; small amounts of cupric oxide appear

in the scale toward the upper ends of the curves shown in the figure. At 2.0 mm., the oxidation is definitely slower in activated oxygen. The analyses and the color of the scales showed that here cupric oxide precipitates at lower penetration values in activated oxygen than in ordinary oxygen. The scale in activated oxygen appears grey in color, indicating the presence of cupric oxide, after 100–200 min. exposure. Hence the retardation may be due to the lower permeability of cupric oxide to reactants, in accordance with its behavior at 500°. This may also be expected from consideration of the lattice structures of both oxides. A similar decrease of the oxidation rate may be effected by raising the pressure from 2.0 to 4.0 mm. without activation; again cupric oxide begins to appear in the scale sooner.

At 690° the activated oxygen influences the oxidation rate only at 0.5 mm. pressure. The oxidation is accelerated considerably. Cupric oxide appears only at larger values of penetration than those represented in Fig. 5. There is no change in the slope of the oxidation curve with precipitation of cupric oxide. The oxidation at 690° begins to follow the parabolic law after a sufficient scale thickness is reached. The initial growth is slower than that predicted by the parabolic law and the rate constant which is ultimately established. The straight portion of the curve for 0.5 mm. lies outside of the plot in Fig. 5 (compare Table III, note *b*). X-Ray pin-hole patterns of specimens oxidized at 690° to various degrees produced no evidence for any texture changes due to activated oxygen. The views of

is thin or by some additional rate limiting process on the boundaries of the oxide phase. However, there is no reason to believe that the diffusion constant of copper ions and vacant sites in cuprous oxide would change significantly in the region of film thickness concerned (5–10 microns); an effect of this kind would seem probable only in oxide films some hundreds of ångström thick. On the other hand, the length of the initial period with the slower growth varies with the oxygen pressure and is consistently decreased by the activated oxygen of various degrees of activation (Fig. 6). The only change introduced into the oxidation process by the activated oxygen is an increase in the number of oxygen atoms striking the surface of the scale per second. It seems, therefore, that the additional rate limiting process during the first stage of cuprous oxide scale growth at 690° and 0.5 mm. pressure is that of the picking up of oxygen in the appropriate form by the surface of the scale. This process has always been considered as an intermediate step in the oxidation of metals,²⁵ but not necessarily rate limiting. At larger scale thicknesses, where the number of copper ions arriving at the surface per second becomes smaller, the pickup of oxygen is fast enough to supply the oxygen atoms necessary to form cuprous oxide. After reaching this stage of growth, further scale growth becomes mainly diffusion-controlled and hence parabolic. By activating the oxygen, more atoms are supplied and the initial slow growth period is correspondingly shortened.

The oxidation rate constants of copper at 600 and 690° are shown in Table III. The constants apply to the straight portions of the curves.

Certain correlations become apparent if all effects observed are considered. Generally, activated oxygen may influence the oxidation of a metal in two ways: (1) it may accelerate or retard the oxidation, and (2) it may change the composition of the oxide scale. Examples of both effects are observed in oxidation of copper. When only cuprous oxide is present in the scale, activating the oxygen as well as increasing the total pressure causes an acceleration of the oxidation. However, at some point in the oxidation the precipitation of cupric oxide begins to interfere with this simple relation. At 500° the activated oxygen does not accelerate the precipitation; at 600° the precipitation is accelerated by activated oxygen. The break in the oxidation curve manifest upon the precipitation of cupric oxide at 500° and vaguely indicated in some runs at 600° is non-existent at 690°. Thus the precipitation decreases the rate constant very definitely at 500°, slightly at 600°, and not at all at 690°. This might be explained by the failure of the slow-growing cupric oxide²² (fine crystals) to form a continuous film on the surface of the cuprous oxide (large crystals). The latter grows slowly at

TABLE III
PARABOLIC OXIDATION RATE CONSTANTS FOR COPPER AT
600 AND 690°

Temp., °C.	Oxygen pressure, mm.	$k \times 10^{10}$ in oxygen ^a	
		Ordinary	Activated
600	0.5	0.35	0.47
	1.0	.49	0.50
	2.0	.64	0.57
	4.0	.62	
	760	.95	
690	0.5	(2.5) ^b	2.8
	1.0	3.8	3.8
	2.0	4.2	4.2

* Rate constant in sq. cm. sec.⁻¹. ^b Obtained from thicker specimens of other origin. In Fig. 5, the region of parabolic scale growth could not be reached on specimens of 50 microns in thickness.

Feitknecht,²² Wilkins and Rideal,²³ and Wagner²⁴ are that the oxidation of copper at these temperatures occurs by lattice diffusion of reactants through the scale. Thus the retarded initial growth at 690° may be caused either by a decreased diffusion constant when the cuprous oxide layer

(22) W. Feitknecht, *Schweiz. Archiv. Angew. Wiss. Techn.*, **6**, 1 (1940).

(23) F. J. Wilkins and E. K. Rideal, *Proc. Roy. Soc. (London)*, **A128**, 394 (1930).

(24) C. Wagner, *Z. angew. Chem.*, **49**, 735 (1936).

(25) E. A. Gulbransen, *Trans. Am. Electrochem. Soc.*, **83**, 301 (1943).

500° but much faster at 690°. Under the microscope, the cupric oxide layer formed at 500° appeared much smoother than layers formed at higher temperatures.

The oxidation rates of other metals studied were not influenced by activating the oxygen. There is some indication that the rate of oxidation of molybdenum at 690° is somewhat retarded by activated oxygen.

It was not possible to correlate, in a quantitative way, the effects caused by activated oxygen with the concentration of free oxygen atoms. Probably the relation between free atom concentration in the gas phase and in the adsorbed layer on the surface of the oxide scale is quite complex.

From (1) measurements of the resistance of copper specimens at experimental temperatures in ordinary and in activated oxygen, (2) theoretical calculations which cannot be presented here because of space limitations, and (3) the fact that activated oxygen was found to accelerate as well as to retard the rate of oxidation, it follows that the effects observed in the oxidation of copper in

activated oxygen are not due merely to the thermal effects of the recombination of oxygen atoms on the surface of the oxide scale.

Acknowledgment.—The author would like to express his appreciation to Dr. M. Kilpatrick, Dr. H. J. McDonald and Dr. D. D. Cubicciotti for encouragement and advice received during the course of this work, and to Dr. J. Whitney for help in the interpretation of the X-ray patterns.

Summary

The oxidation of copper, and several other metals, in ordinary and in activated oxygen are compared. Only in the case of copper are reproducible differences caused by the presence of an excess of free oxygen atoms in oxygen. Cases in which the monatomic oxygen accelerates, retards or does not influence the rate of oxidation are described. The conditions for the appearance of cupric oxide in the scale are outlined and an explanation of some types of complex oxidation curves is attempted.

CHICAGO, ILLINOIS

RECEIVED JULY 11, 1949

[CONTRIBUTION FROM THE GATES AND CRELLIN LABORATORIES OF CHEMISTRY, CALIFORNIA INSTITUTE OF TECHNOLOGY, No. 1433]

The Distribution of Ferric Iron between Hydrochloric Acid and Isopropyl Ether Solutions. I. The Compound Extracted and the Extraction at Constant Acid Concentration

BY ROLLIE J. MYERS, DAVID E. METZLER AND ERNEST H. SWIFT

Introduction

This series of papers presents the results of a continuation of the experimental work which has been in progress in this Laboratory on the distribution of certain inorganic compounds between immiscible liquid phases.

Dodson, Forney and Swift¹ have demonstrated that isopropyl ether could be used for the quantitative extraction of ferric iron from hydrochloric acid solutions; that the distribution of the iron was greatly dependent upon the acid concentration; and that, within certain limits, extraction was increased by an increase in acid concentration. They also observed that at a constant acid concentration the per cent. of iron extracted decreased when the total amount of iron present was decreased and that under certain conditions two ether phases were formed. This investigation was undertaken to examine the distribution process more closely, and especially to study these last two phenomena. During the preparation of these articles for publication a similar study was published.² Although the general experimental results are similar, our interpretation in some cases

is different. Attention will be called to these differences in the subsequent articles.

Experimental Procedures

Distribution Procedure.—The aqueous hydrochloric acid-iron solutions were prepared in 25-ml. volumetric flasks. The contents of a flask was transferred to a 50-ml. ground-glass stoppered mixing cylinder and 25 ml. of ether was added. These cylinders were then shaken vigorously and placed in a thermostat regulated at $25.0 \pm 0.02^\circ$. The cylinders were shaken vigorously for one minute at fifteen-minute intervals during one hour, then were shaken twice in ten minutes, and allowed to settle for at least five minutes, usually longer, before samples were removed.

The samples were removed from both layers with pipets, experiments having shown that the ether drainage did not introduce a significant error. For the analysis of iron in the ether layer the ether was removed by evaporation, or the iron was extracted by shaking the ether with several portions of water.

Analysis for Iron.—For quantities of iron greater than 0.5 millimole the iodometric procedure described by Swift³ was used. For quantities less than 0.5 millimole and greater than 0.01 millimole this procedure was modified by bringing a 20-ml. portion of solution containing 24–48 millimoles of hydrochloric acid to a boil, flushing out the air with carbon dioxide, then stoppering the flask. The flask was at least twice more flushed with carbon dioxide while cooling. When cool, 3 g. of potassium iodide was added to the sample and the solution allowed to stand for one minute. Then 100 ml. of water was added and the solution was titrated with 0.01 *N* (volume formal) sodium thiosulfate to

(1) R. W. Dodson, G. J. Forney and E. H. Swift, *This Journal*, **58**, 2573 (1936).

(2) N. H. Nachtrieb and J. G. Conway, *ibid.*, **70**, 3547 (1948), and N. H. Nachtrieb and R. E. Fryxell, *ibid.*, **70**, 3552 (1948).

(3) E. H. Swift, *ibid.*, **53**, 2682 (1929).